Monthly Notices of the ROYAL ASTRONOMICAL SOCIETY
MNRAS **449,** 1954–1966 (2015) doi:10.1093/mnras/stv335

Massive stars exploding in a He-rich circumstellar medium – VI. Observations of two distant Type Ibn supernova candidates discovered by La Silla-QUEST

A. Pastorello,[1⋆] E. Hadjiyska,[2] D. Rabinowitz,[2] S. Valenti,[3,4] M. Turatto,[1] G. Fasano,[1] S. Benitez-Herrera,[5] C. Baltay,[2] S. Benetti,[1] M. T. Botticella,[6] E. Cappellaro,[1] N. Elias-Rosa,[1] N. Ellman,[2] U. Feindt,[7] A. V. Filippenko,[8] M. Fraser,[9] A. Gal-Yam,[10] M. L. Graham,[8] D. A. Howell,[3,4] C. Inserra,[11] P. L. Kelly,[8] R. Kotak,[11] M. Kowalski,[7] R. McKinnon,[2] A. Morales-Garoffolo,[12] P. E. Nugent,[8,13] S. J. Smartt,[11] K. W. Smith,[11] M. D. Stritzinger,[14] M. Sullivan,[15] S. Taubenberger,[5,16] E. S. Walker,[2] O. Yaron[10] and D. R. Young[11]

Affiliations are listed at the end of the paper

Accepted 2015 February 16. Received 2015 February 16; in original form 2014 August 19

ABSTRACT

We present optical observations of the peculiar stripped-envelope supernovae (SNe) LSQ12btw and LSQ13ccw discovered by the La Silla-QUEST survey. LSQ12btw reaches an absolute peak magnitude of $M_g = -19.3 \pm 0.2$, and shows an asymmetric light curve. Stringent pre-discovery limits constrain its rise time to maximum light to less than 4 d, with a slower post-peak luminosity decline, similar to that experienced by the prototypical SN Ibn 2006jc. LSQ13ccw is somewhat different: while it also exhibits a very fast rise to maximum, it reaches a fainter absolute peak magnitude ($M_g = -18.4 \pm 0.2$), and experiences an extremely rapid post-peak decline similar to that observed in the peculiar SN Ib 2002bj. A stringent pre-discovery limit and an early marginal detection of LSQ13ccw allow us to determine the explosion time with an uncertainty of ±1 d. The spectra of LSQ12btw show the typical narrow He I emission lines characterizing Type Ibn SNe, suggesting that the SN ejecta are interacting with He-rich circumstellar material. The He I lines in the spectra of LSQ13ccw exhibit weak narrow emissions superposed on broad components. An unresolved Hα line is also detected, suggesting a tentative Type Ibn/IIn classification. As for other SNe Ibn, we argue that LSQ12btw and LSQ13ccw likely result from the explosions of Wolf–Rayet stars that experienced instability phases prior to core collapse. We inspect the host galaxies of SNe Ibn, and we show that all of them but one are hosted in spiral galaxies, likely in environments spanning a wide metallicity range.

Key words: supernovae: general – supernovae: individual: LSQ12btw – supernovae: individual: LSQ13ccw – supernovae: individual: SN 2006jc – supernovae: individual: SN 2011hw.

1 INTRODUCTION

The discoveries of SN 1999cq (Matheson et al. 2000) and, a few years later, the well-studied SN 2006jc (e.g. Foley et al. 2007; Pastorello et al. 2007) revealed the existence of a new group of core-collapse supernovae (CCSNe) with peculiar observational properties: a relatively high peak luminosity ($M_R \approx -19$ mag), blue colours and spectra showing relatively narrow (a few thousand km s^{-1}) emission lines of He I superposed on typical Type Ic supernova (SN Ic; e.g. Filippenko 1997) spectral features. These observables have been interpreted as signatures of interaction between the SN ejecta and a circumstellar medium (CSM) rich in He (Chugai 2009, and references therein). Very few SNe of this family (named

⋆E-mail: andrea.pastorello@oapd.inaf.it

Type Ibn SNe; Pastorello et al. 2008a) were discovered in the past, but their number has significantly grown in recent years, reaching the current number of 16. These new discoveries are showing that a wide degree of heterogeneity exists in the properties of SNe Ibn. A number of papers studying a variety of SNe Ibn have been published so far,[1] and observations of three recent, unusual SNe Ibn (SN 2010al, SN 2011hw and OGLE-2013-SN-006) are published in two companion papers of our team (Pastorello et al. 2015a,b). It is interesting to note that SN 2011hw, along with another object studied some years ago (SN 2005la), showed clear evidence of H lines (Pastorello et al. 2008b, 2015a; Smith et al. 2012; Bianco et al. 2014; Modjaz et al. 2014), indicating that their CSM was also moderately H-rich. This led researchers to the conclusion that there is a continuity in properties between SNe Ibn and SNe IIn (e.g. Smith et al. 2012).

Because of their rarity, early discovery of new members of this class offers an opportunity for improving our understanding of their physical nature. In this respect, the currently running programmes for the prompt spectroscopic classification of new SN candidates – such as the Public ESO Spectroscopic Survey for Transient Objects (PESSTO; Smartt et al. 2013) and the Asiago Classification Program (Tomasella et al. 2014) – play an important role in providing new SNe Ibn as well as other types of unusual transients.

This paper describes our data set for two new peculiar stripped-envelope SNe that we propose to be SNe Ibn, and discusses them in the context of what is currently known on the subject.

LSQ12btw and LSQ13ccw were found by the La Silla-QUEST (LSQ) survey (Hadjiyska et al. 2011; Baltay et al. 2013) and tentatively classified as SN 2006jc-like (Type Ibn) SNe by the PESSTO Collaboration (Valenti et al. 2012; Kangas et al. 2013). The former object was discovered on 2012 April 9.04 (UT dates are used throughout this paper), close to the nucleus of the spiral, star-forming galaxy the Sloan Digital Sky Survey (SDSS) J101028.69+053212.5 (see Fig. 1). SDSS DR3 reports a redshift $z = 0.057\,64 \pm 0.000\,06$.[2] Adopting a Hubble constant $H_0 = 73\ \mathrm{km\ s^{-1}\ Mpc^{-1}}$ ($\Omega_M = 0.27$ and $\Omega_\Lambda = 0.73$), we infer a luminosity distance of about 247 ± 16 Mpc ($\mu = 36.97 \pm 0.15$ mag). No sign of interstellar absorption within the host galaxy is visible in the SN spectra (see Section 2.2), so we consider only the Galactic extinction component for LSQ12btw, $A_g = 0.075$ mag (Schlafly & Finkbeiner 2011).

LSQ13ccw was discovered on 2013 September 4.03 near the galaxy 2MASX J21355077−1832599 (also known as PGC 866755; Fig. 1). The redshift of the host galaxy was measured through the SN features and the detection of weak and narrow lines of [O III] λλ4959, 5007 from the galaxy. These give $z = 0.0603 \pm 0.0002$ and a luminosity distance of 259 ± 17 Mpc ($\mu = 37.07 \pm 0.14$ mag). Since there is no clear spectroscopic evidence (see Section 2.2) of host-galaxy absorption, we again adopt only the Milky Way component ($A_g = 0.163$ mag) as total line-of-sight absorption to LSQ13ccw.

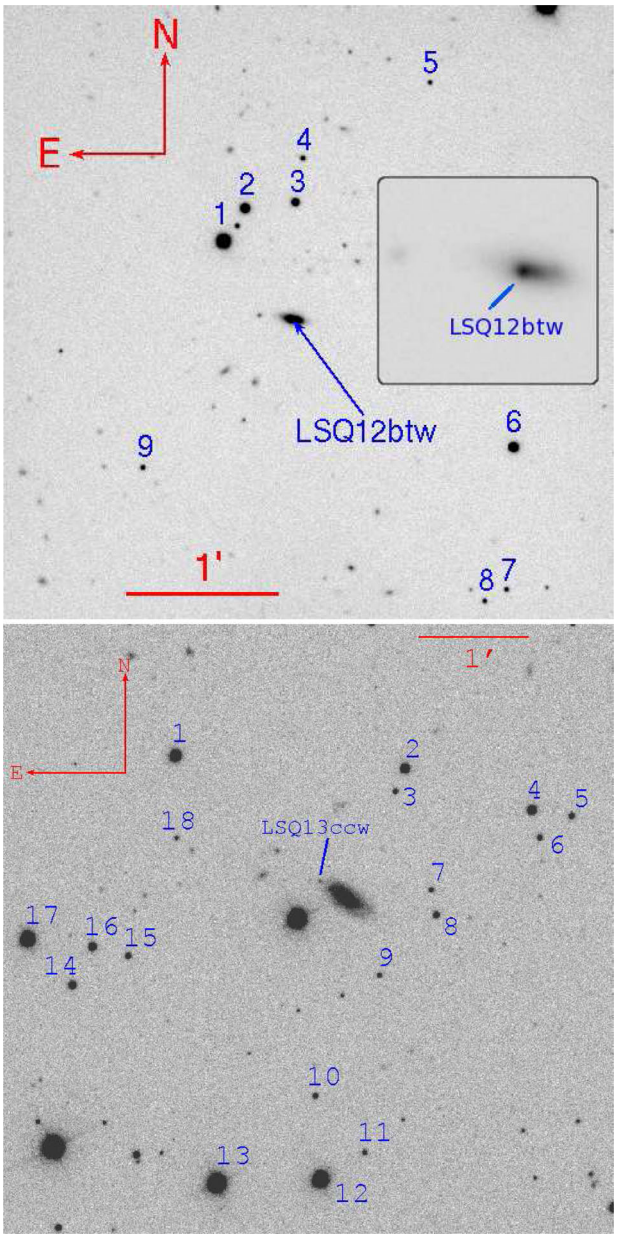

Figure 1. Top: ESO-NTT *r*-band image of LSQ12btw obtained on 2012 March 14. The inset at right shows the nuclear region of the host galaxy with a different cut level, highlighting the presence of the SN, due east of the galaxy nucleus. Bottom: LT *V*-band image of LSQ13ccw and its host galaxy obtained on 2013 September 22. The numbers mark the SDSS reference stars used to calibrate the magnitudes of the two SNe.

2 OBSERVATIONS

2.1 Photometry

The field of LSQ12btw was repeatedly monitored over the past few years by LSQ and Pan-STARRS1 (PS1; see Inserra et al. 2013, for a description of the PS1 3Pi survey, exposure times, and depths). As we will discuss later in this section, there is no previous detection of variability at the SN position. The most recent LSQ image with no detection was obtained on 2012 March 23.12 (JD = 245 6009.62), while images on March 27.11 (JD = 245 6013.61) clearly showed

[1] Additional publications on this subject include Pastorello et al. (2008a, 2008b), Mattila et al. (2008), Smith, Foley & Filippenko (2008), Immler et al. (2008), Di Carlo et al. (2008), Nozawa et al. (2008), Tominaga et al. (2008), Anupama et al. (2009), Sakon et al. (2009), Smith et al. (2012), Sanders et al. (2013), Modjaz et al. (2014), Bianco et al. (2014) and Gorbikov et al. (2014).

[2] The spectroscopic data were obtained on 2004 September 28; http://www.sdss.org/dr3/products/spectra/getspectra.html.

Table 1. Sloan *g*, *r*, *i* and *z* photometry of LSQ12btw, and associated uncertainties.

Date	JD	Phase[a]	*V*	*g*	*r*	*i*	*z*	Inst.
13-02-2012	245 5970.97	−39.0		–	>22.89	>22.26	–	1
20-02-2012	245 5978.02	−32.0		>22.74	–	–	–	1
16-03-2012[b]	245 6002.84	−7.2	[>21.42]	–	>21.24	–	–	1
19-03-2012[b]	245 6005.87	−4.1	[>21.96]	–	>21.77	–	–	1
23-03-2012[c]	245 6009.62	−0.4	[>21.77]	>21.89	–	–	–	2
27-03-2012[c]	245 6013.61	+3.6	[17.93 0.05]	17.76 0.04	–	–	–	2
28-03-2012[c]	245 6014.61	+4.6	[18.06 0.05]	17.93 0.04	–	–	–	2
07-04-2012[c]	245 6024.54	+14.5	[18.72 0.11]	18.70 0.08	–	–	–	2
07-04-2012[c]	245 6024.63	+14.6	[18.64 0.09]	18.62 0.07	–	–	–	2
09-04-2012[c]	245 6026.54	+16.5	[18.87 0.07]	18.86 0.05	–	–	–	2
09-04-2012[c]	245 6026.62	+16.6	[18.84 0.08]	18.82 0.06	–	–	–	2
12-04-2012	245 6029.59	+19.6		19.08 0.20	–	–	–	3
12-04-2012	245 6029.80	+19.8		19.09 0.13	–	–	–	1
14-04-2012	245 6031.58	+21.6		19.15 0.12	19.12 0.18	19.23 0.21	–	3
19-04-2012[c]	245 6036.52	+26.5	[19.70 0.07]	19.77 0.06	–	–	–	2
19-04-2012[c]	245 6036.61	+26.6	[19.77 0.08]	19.84 0.06	–	–	–	2
21-04-2012	245 6038.67	+28.7		19.99 0.08	19.88 0.06	20.07 0.06	–	3
22-04-2012	245 6040.39	+30.4		20.22 0.24	20.05 0.27	20.22 0.27	19.85 0.30	4
30-04-2012	245 6047.58	+37.5		20.57 0.41	20.79 0.52	–	–	3
03-05-2012[c]	245 6050.57	+40.6	[21.05 0.77]	20.91 0.60	–	–	–	2
08-05-2012	245 6056.40	+46.4		20.93 0.04	21.23 0.10	22.12 0.18	21.02 0.25	5
23-05-2012	245 6071.45	+61.5		21.50 0.19	22.08 0.33	22.77 0.29	–	6

Notes. Measurements from LSQ and PS1 wide broad-band images were first scaled to Sloan *g* and Sloan *r* magnitudes, respectively, and then transformed to Johnson *V*-band magnitudes by applying the relations of Jester et al. (2005) for blue stars (see text). When no source was detected at the SN position, 3σ detection limits are reported. PS1 photometry was obtained from the combined images after co-adding two single exposures. Indicated errors account for both the uncertainties in the photometric measurement and the final zero-point calibration.
1 = 1.8-m PS1 Telescope + GPC1; 2 = 1.0-m ESO Schmidt Telescope + LSQ Camera; 3 = 3.58-m ESO NTT + ESO Faint Object Spectrograph and Camera v.2 (EFOSC2); 4 = 2.0-m LT + RATCam; 5 = 3.58-m Telescopio Nazionale Galileo (TNG) + Dolores; and 6 = 10.4-m Gran Telescopio Canarias (GTC) + Osiris.
[a]Days from the time of the shock breakout;
[b]PS1 w_{P1}-filter data converted to Sloan *r* and Johnson *V* magnitudes;
[c]LSQ Q_{st}-filter data converted to Sloan *g* and Johnson *V* magnitudes.

the new source. This allows us to constrain the epoch of shock breakout to JD = 245 6010.0$^{+3.6}_{-1.0}$.

Even more stringent is the constraint on the explosion epoch for LSQ13ccw. The object was not detected on 2013 August 29.10 (JD = 245 6533.60), while there are two marginal detections on 2013 August 31.02 and 31.10 (JD = 245 6535.52 and 245 6535.60). Two additional images were obtained on September 4, showing the object at peak luminosity. The fast rise to maximum and the marginal detections of August 31 allow us to constrain the time of shock breakout with a small uncertainty, JD = 245 6534.5 ± 1.0.

Photometric data for LSQ12btw and LSQ13ccw were obtained with Sloan filters, using different instruments available to our collaboration (see footnotes of Tables 1 and 2 for details). The data were reduced following standard prescriptions in the IRAF[3] environment (including bias, overscan, flat-field correction and final trimming). Additional Johnson *B*- and *V*-band observations were obtained for LSQ13ccw using Las Cumbres Observatory Global Telescope (LCOGT) facilities and the Liverpool Telescope (LT). Standard fields from the Landolt (1992) and Smith et al. (2002) catalogues were observed during a few photometric nights, and were used to calibrate the magnitudes of several stars (used as local standards; Fig. 1) in the fields of the two SNe. The magnitudes of each of the two transients were calibrated relative to the average magnitudes of the respective sequences of local standards.

Most PS1 and LSQ observations were obtained through very broad filters.[4] The magnitudes in the original photometric systems of the two telescopes were scaled to Sloan *g* (LSQ) and Sloan *r* (PS1) using the magnitudes of Sloan reference stars and the transmission-curve information of the two non-standard wide passband filters. Finally, Sloan *g* or *r* magnitudes were converted to Johnson *V* by applying the transformation relations of Jester et al. (2005) for blue stars, and using the $g - r$ colour information inferred from photometry obtained on adjacent nights and from the available spectra. The final magnitudes of LSQ12btw and LSQ13ccw are reported in Tables 1 and 2, respectively, and their multiband light curves are shown in Fig. 2.

The light curves of LSQ12btw are asymmetric, with a fast (≤4 d) rise to maximum light, and a slower post-peak decline. None the less, in analogy to SN 2006jc (Pastorello et al. 2008a), the

[3] IRAF is distributed by the National Optical Astronomy Observatory, which is operated by the Association of Universities for Research in Astronomy (AURA), Inc., under cooperative agreement with the US National Science Foundation (NSF).

[4] The broad interference filter used by the LSQ survey, labelled as Q_{st}, has an almost constant transmission between 460 and 700 nm (see fig. 2 of Baltay et al. 2013), while the w_{P1} PS1 filter has a flat transmission between ∼410 and 805 nm (Tonry et al. 2012).

Table 2. Sloan g, r, i and z photometry, and Johnson–Bessell B and V photometry, of LSQ13ccw, and associated uncertainties.

Date	JD	Phase[a]	B	V	g	r	i	Inst.
24-08-2013	245 6528.94	−5.6	–	–	–	–	>22.26	1
25-08-2013[c]	245 6529.51	−5.0	–	[>22.08]	>22.11	–	–	2
25-08-2013[c]	245 6529.59	−4.9	–	[>22.21]	>22.24	–	–	2
29-08-2013[c]	245 6533.52	−1.0	–	[>22.23]	>22.26	–	–	2
29-08-2013[c]	245 6533.60	−0.9	–	[>23.06]	>23.09	–	–	2
31-08-2013[c,b]	245 6535.52	+1.0	–	[22.26 0.63]	22.32 0.63	–	–	2
31-08-2013[c,b]	245 6535.60	+1.1	–	[22.10 0.59]	22.16 0.59	–	–	2
31-08-2013	245 6535.87	+1.4	–	–	20.68 0.09	20.55 0.10	–	1
04-09-2013[c]	245 6539.53	+5.0	–	[18.85 0.09]	18.88 0.07	–	–	2
04-09-2013[c]	245 6539.63	+5.1	–	[18.91 0.08]	18.94 0.06	–	–	2
06-09-2013[c]	245 6541.53	+7.0	–	[19.12 0.07]	19.18 0.05	–	–	2
06-09/2013[c]	245 6541.62	+7.1	–	[19.15 0.07]	19.21 0.05	–	–	2
06-09-2013	245 6541.85	+7.4	–	–	19.22 0.14	–	–	1
06-09-2013	245 6542.35	+7.9	19.37 0.06	19.27 0.10	19.16 0.04	19.20 0.12	19.17 0.11	3
07-09-2013	245 6542.99	+8.5	19.45 0.18	19.32 0.23	19.41 0.10	19.35 0.19	19.36 0.20	4
08-09-2013[c]	245 6543.53	+9.0	–	[19.53 0.07]	19.59 0.05	–	–	2
08-09-2013[c]	245 6543.64	+9.1	–	[19.57 0.07]	19.63 0.04	–	–	2
09-09-2013	245 6544.62	+10.1	–	19.70 0.06	–	–	–	5
10-09-2013[c]	245 6545.54	+11.0	–	[19.82 0.07]	19.92 0.05	–	–	2
10-09-2013	245 6545.60	+11.1	20.04 0.13	19.95 0.11	19.88 0.04	19.73 0.06	19.58 0.08	6
10-09-2013[c]	245 6545.65	+11.2	–	[19.91 0.06]	20.02 0.04	–	–	2
10-09-2013	245 6546.35	+11.9	20.18 0.20	20.00 0.32	–	–	–	3
11-09-2013	245 6546.60	+12.1	20.21 0.37	–	20.13 0.14	19.99 0.19	19.88 0.24	7
11-09-2013	245 6547.35	+12.9	20.36 0.25	–	–	–	–	3
12-09-2013[c]	245 6547.54	+13.0	–	[20.34 0.11]	20.43 0.10	–	–	2
12-09-2013[c]	245 6547.64	+13.1	–	[20.33 0.09]	20.42 0.08	–	–	2
12-09-2013	245 6548.37	+13.9	20.53 0.16	–	–	–	–	8
18-09-2013	245 6553.88	+19.4	20.85 0.40	–	20.80 0.43	20.82 0.54	20.82 0.33	9
19-09-2013	245 6554.96	+20.5	21.01 0.21	20.86 0.20	20.95 0.25	20.98 0.45	20.89 0.26	9
20-09-2013	245 6555.93	+21.4	21.17 0.17	21.01 0.40	21.14 0.10	21.10 0.18	21.01 0.18	9
20-09-2013	245 6556.39	+21.9	21.21 0.32	21.03 0.27	–	–	–	10
21-09-2013	245 6557.41	+22.9	21.32 0.23	21.16 0.15	–	–	–	10
22-09-2013	245 6558.40	+23.9	21.57 0.10	21.25 0.12	–	–	–	10
23-09-2013	245 6558.99	+24.5	–	–	>20.57	21.45 0.41	21.43 0.36	9
23-09-2013	245 6559.39	+24.9	21.75 0.10	21.41 0.20	–	–	–	10
24-09-2013	245 6560.40	+25.9	21.94 0.15	–	–	–	–	10
26-09-2013	245 6562.40	+27.9	22.17 0.21	21.80 0.19	–	–	–	10
27-09-2013	245 6563.38	+28.9	22.32 0.11	21.94 0.23	–	–	–	10
28-09-2013	245 6564.37	+29.9	22.45 0.18	22.17 0.18	–	–	–	10
29-09-2013	245 6565.37	+30.9	22.58 0.09	22.27 0.18	–	–	–	10
01-10-2013	245 6567.39	+32.9	22.90 0.19	22.59 0.24	–	–	–	10
04-10-2013	245 6570.39	+35.9	23.37 0.43	23.09 0.33	–	–	–	10
06-10-2013	2456572.41	+37.9	23.70 0.24	23.34 0.42	–	–	–	10
07-10/2013	2456573.38	+38.9	–	–	23.80 0.45	23.66 0.52	22.92 0.57	10

Notes. Measurements from LSQ Q_{st} wide broad-band images were first scaled to Sloan g magnitudes, and then transformed to Johnson V-band magnitudes by applying the relations of Jester et al. (2005) for blue stars (see text). When no source is detected at the SN position, 3σ detection limits are reported. Indicated errors account for both the uncertainties in the photometric measurement and the final zero-point calibration.

1 = 1.8-m PS1 Telescope + GPC1; 2 = 1.0-m ESO Schmidt Telescope + LSQ Camera; 3 = LCOGT 1m0-13 (SAAO); 4 = LCOGT 1m0-03 (SSO); 5 = 3.58-m NTT + EFOSC2 6 = LCOGT 1m0-09 (CTIO); 7 = LCOGT 1m0-04 (CTIO); 8 = LCOGT 1m0-12 (SAAO); 9 = 2.0-m Faulkes Telescope South + fs03; 10 = 2.0-m LT + I0:0.

[a]Days from the time of the shock breakout; [b]2σ detection;

[c]LSQ Q_{st}-filter photometry is converted to Sloan g and Johnson V magnitudes.

decline of the light curve of LSQ12btw is much steeper (on average, $\gamma_V = 8.4 \pm 0.3$ mag/100 d) than those observed in canonical SNe Ib/c. We also note that, at phases >30 d, the decline slightly slows down, possibly marking the transition to the nebular phase. The light curve of LSQ13ccw shows a very rapid rise to maximum light similar to that of LSQ12btw, and a surprisingly fast average decline $\gamma_V = 13.3 \pm 0.2$ mag/100 d. The light curve of LSQ13ccw is remarkably similar to that of the peculiar SN Ib 2002bj (Poznanski et al. 2010, cf. Section 3). With the distances and reddening values adopted in Section 1, the absolute peak magnitudes of LSQ12btw and LSQ13ccw are $M_g = -19.3 \pm 0.2$ and $M_g = -18.4 \pm 0.2$, respectively.

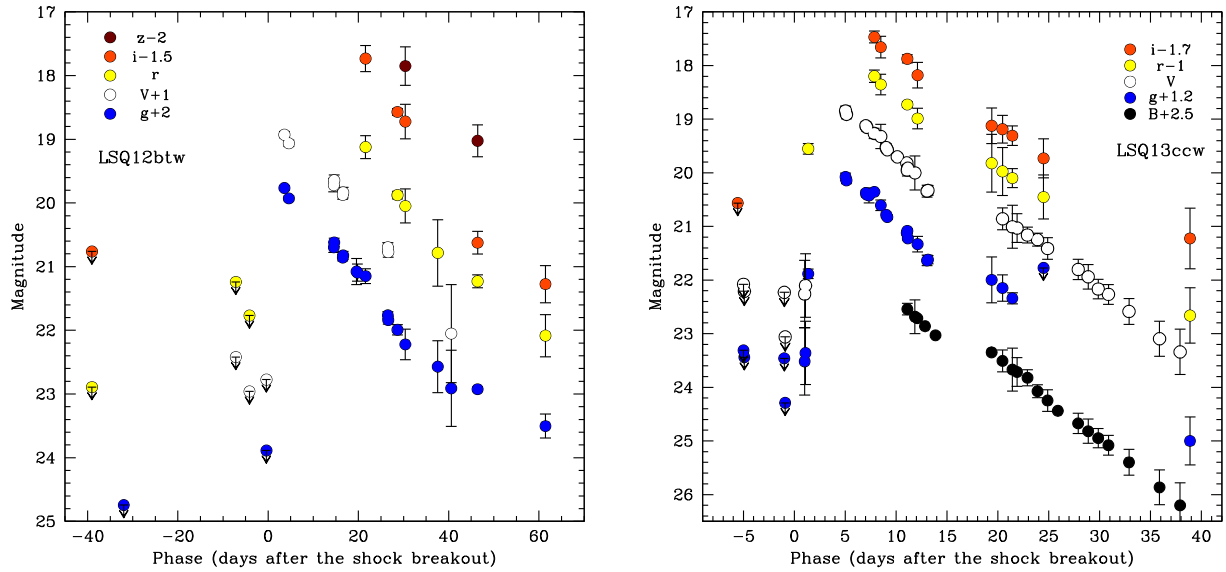

Figure 2. Left: optical light curves of LSQ12btw. Right: optical light curves of LSQ13ccw. *B* and *V* light curves were calibrated using the Landolt (1992) catalogue (Vegamag system), while *g*, *r*, *i* and *z* light curves were calibrated using the Sloan catalogue (ABmag system).

One of the most compelling observational results in recent years is the discovery of outbursts occasionally occurring a short time (weeks to years) before the explosion of interacting SNe (e.g. Pastorello et al. 2007; Fraser et al. 2013b; Mauerhan et al. 2013; Ofek et al. 2013). We searched for evidence of pre-SN activity in archival images of both LSQ12btw and LSQ13ccw. We inspected deep images of the field of LSQ12btw obtained by the LSQ survey (limiting magnitude of about 22), and by PS1 (limiting magnitude of ∼20) in 2010 March. Deep PS1 and LSQ images were also obtained in 2012 March. All these archive images showed no source detected at the SN position. PS1 observed the position of LSQ13ccw on 19 occasions (when the object fell on good pixels) between 2009 June and seven days before our first discovery epoch in the various *grizy* filters of PS1. LSQ images were collected from 2012 May to 2012 September, and from 2013 April to August. No pre-SN eruption of LSQ13ccw was detected. Although PS1 and LSQ have made serendipitous discoveries (see e.g. Fraser et al. 2013b), the lack of detections at the position of LSQ13ccw and LSQ12btw does not rule out that such outbursts occurred, since the temporal coverage is sparse and the detection limits are not deep enough to detect intrinsically faint transients. This can be visualized by comparing the pre-discovery detection limits of the two SNe with observations of the fields of two well-studied objects showing signs of pre-SN activity: the Type Ibn SN 2006jc in UGC 4904 and the Type IIn SN 2009ip in NGC 7259 (Fig. 3). The pre-SN outbursts of SN 2006jc and 2009ip reached an absolute magnitude of about −14, which is below the detection threshold of almost all our observations of LSQ12btw and LSQ13ccw.

2.2 Spectroscopy

The faint apparent magnitudes coupled with the rapid evolution did not allow extensive spectroscopic coverage of these two SNe. We obtained two spectra of LSQ12btw and one of LSQ13ccw with the 3.58-m New Technology Telescope (NTT) of the European Southern Observatory (ESO, La Silla, Chile) equipped with EFOSC2, plus an additional spectrum of LSQ13ccw with the 10-m Keck-II telescope equipped with the DEIMOS spectrograph. Spectra of the two SNe, and the flux standard stars were obtained with the slit oriented along the parallactic angle (Filippenko 1982). Information on the spectroscopic observations is reported in Table 3. All spectra[5] are shown in Fig. 4, along with those of the Type Ibn SN 2006jc (Pastorello et al. 2007), the transitional SN Ibn/IIn 2011hw (Pastorello et al. 2015a) and a spectrum of the peculiar Type Ib SN 2002bj (Poznanski et al. 2010).

The first spectrum of LSQ12btw, obtained on 2012 April 12 (∼20 d after the shock breakout), is the classification spectrum announced by Valenti et al. (2012). The second spectrum was collected on April 21 (∼+29 d). Between the two epochs there was little evolution, with the latter spectrum being slightly redder than the former. Both show a blue pseudo-continuum, with a drop in the flux above 5700 Å. This pseudo-continuum is a common feature in Type Ibn and other interacting SNe, and has been attributed to blends of Fe II emission lines formed in the shocked material (Smith et al. 2009, 2012). The spectrum shows many of the lines observed in SNe IIn (Fig. 4),[6] including the broad bump at 6300–6400 Å (possibly due to a blend of Si II λ6355, Mg II λ6346, and/or (less likely) [O I] λλ6300, 6364). Another feature at about 7800 Å is clearly detected, probably a line blend including O I λ7774. The near-infrared (NIR) Ca II triplet, prominent in SN 2006jc (Pastorello et al. 2007), is weak or absent. But the most remarkable features are the emissions lines of He I, with a velocity of 4000–4500 km s^{-1}, as measured from the full width at half-maximum intensity (FWHM) of the He I λ5876 line.[7]

[5] These spectra are available from WISeREP (Yaron & Gal-Yam 2012).

[6] The comprehensive line identification, based on the features observed in the higher quality spectrum of SN 2006jc, is shown in Fig. 4 (Pastorello et al. 2007; Anupama et al. 2009).

[7] Although we admit that lines with $v_{\rm FWHM} \approx$ 4000–4500 km s^{-1} cannot be formally considered to be 'narrow', here we consider these velocities as lying in the range of values that are observed in SN Ibn spectra. This is because wind velocities of a few thousand km s^{-1} are not infrequent in Wolf–Rayet stars. In addition, spectra of well-monitored SNe Ibn such as SN 2010al (Pastorello et al. 2015a) exhibit an FWHM velocity for the He I lines that grows with time, suggesting an increasing contribution of ejecta/CSM shocked material to the line flux.

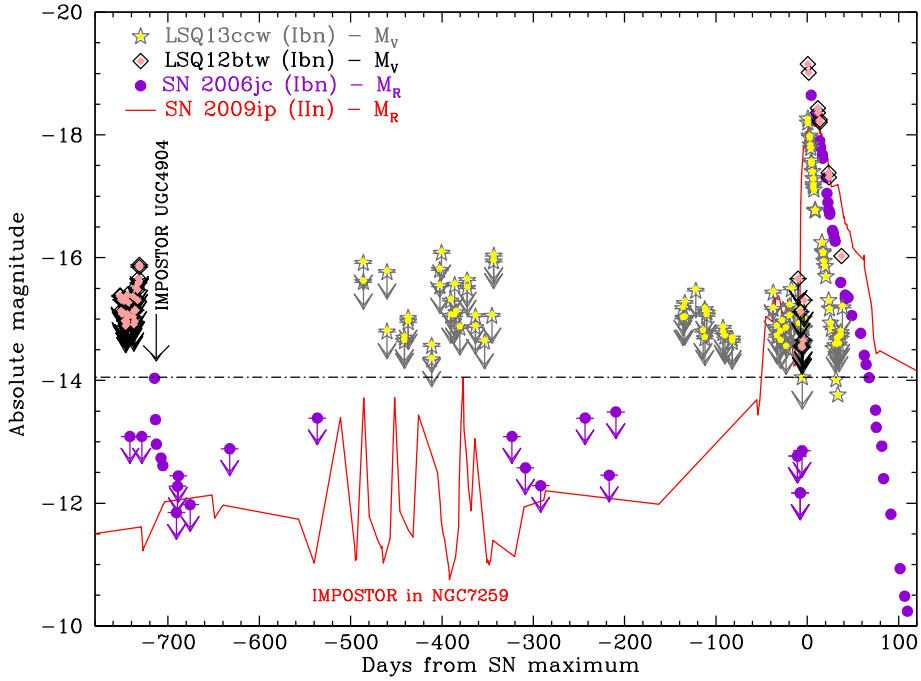

Figure 3. Absolute *V*-band light curves of LSQ12btw and LSQ13ccw, compared with the *R*-band observations of the Type Ibn SN 2006jc and the Type IIn SN 2009ip. These observations include detection limits, pre-SN outbursts, and SN light curves. Data for SN 2006jc are from Pastorello et al. (2007, 2008a), while those for SN 2009ip are from Pastorello et al. (2013), Fraser et al. (2013a), Margutti et al. (2014) and Graham et al. (2014). The horizontal dot–dashed line indicates the peak magnitudes of typical SN impostors (e.g. Van Dyk et al. 2000; Maund et al. 2006; Tartaglia et al. 2015).

Table 3. Log of spectroscopic observations of LSQ12btw and LSQ13ccw.

Object	Date	JD	Phase	Instrument configuration	Range (Å)	Resolution (Å)
LSQ12btw	12-04-2012	245 6029.60	+19.6	NTT + EFOSC2 + gr.13	3650–9250	18
LSQ12btw	21-04-2012	245 6038.61	+28.6	NTT + EFOSC2 + gr.11 + gr.16	3350–10,000	13,13
LSQ13ccw	09-09-2013	245 6544.63	+10.1	NTT + EFOSC2 + gr.13	3650–9250	18
LSQ13ccw	10-09-2013	245 6545.90	+11.4	Keck II + DEIMOS + gt.600 l/mm	4450–9650	3.7

Note. Phases are in days from shock breakout. The resolution is measured from the FWHM of the night-sky lines.

We also identify narrow, unresolved Hα, Hβ, [O II] λ3727, [O III] λ5007, [N II] λ6584 and [S II] $\lambda\lambda$6717, 6731 emissions, which may originate in the interstellar gas unrelated with the SN, or in the slow-moving, unshocked CSM of LSQ12btw. We favour the former explanation, since the SDSS DR8 spectrum of the host galaxy[8] also exhibits these emission features. This is also supported by the facts that the flux ratios between the putative galaxy lines remain approximately constant in the pre-SN SDSS spectrum of the host galaxy and in the two spectra of LSQ12btw, and that the narrow Hα is spatially more extended than the emission attributed to the SN (see appendix, Fig. A1).

Two spectra of LSQ13ccw were obtained at similar epochs, on 2013 September 9 ($\sim$10.1 d after the adopted explosion time; this spectrum has poor signal-to-noise) and September 10 ($\sim$11.4 d). The spectra are very similar, showing a relatively blue continuum with undulations at the shorter wavelengths that can be attributed to Fe II lines. At about 5880 Å (rest wavelength), we note a broad feature ($v_{\rm FWHM} \approx$ 9000–10 000 km s^{-1}) with a narrower P-Cygni profile superimposed, very likely a blend of Na ID and He I λ5876. This narrow feature indicates the presence of material moving at a relatively low speed ($v \approx$ 3400 km s^{-1}). Additional broad bumps are detected between 6500 and 6700 Å (a blend containing C II $\lambda\lambda$6578, 6583, He I λ6678 and possibly Hα), at about 7200 Å (a line blend of different species, probably including [Ca II] $\lambda\lambda$7291, 7323, C II $\lambda\lambda$7231, 7236, He I λ7065 and He I λ7281), and at $\sim$7800 Å, observed also in LSQ12btw spectra, and identified as O I λ7774.

The identification of typical He I lines such as $\lambda\lambda$7065 and 7281 cannot be firmly confirmed in the two spectra of LSQ13ccw, likely because of blending with lines of other ions, and the presence of a broad telluric absorption band which also may affect the profile of the observed features. However, the blue pseudo-continuum and the detection of fairly narrow He I $\lambda\lambda$4471, 5016 and 5876 lines superposed on broader components suggest that the ejecta are interacting with He-rich CSM, hence supporting the Type Ibn SN classification. In Fig. 5, we show the profiles of strong He I lines and the feature at about 6590 Å in the 2013 September 9 Keck-II spectrum of LSQ13ccw, along with those of the 2012 April 12 NTT spectrum of LSQ12btw. We remark

[8] http://skyserver.sdss3.org/dr8/en/

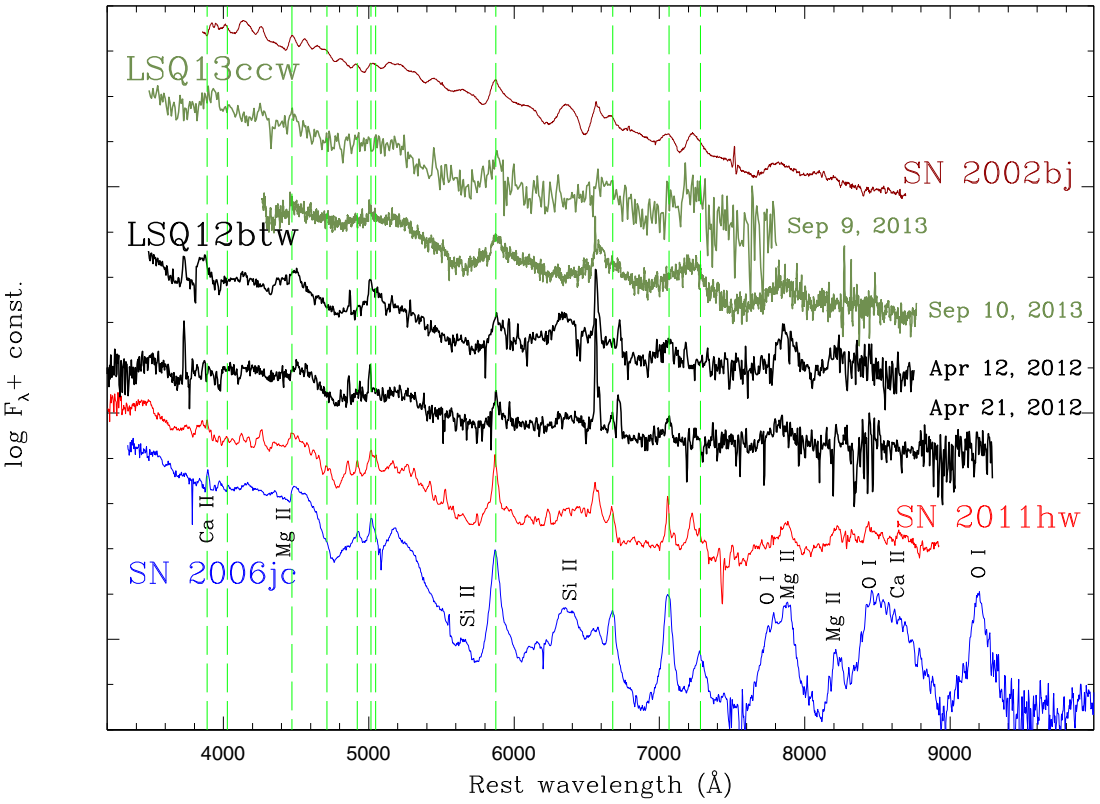

Figure 4. Post-peak spectra of LSQ12btw and LSQ13ccw are compared with those of the Type Ibn SNe 2011hw (Pastorello et al. 2015a) and 2006jc (Pastorello et al. 2007), and of the peculiar SN 2002bj (Poznanski et al. 2010). The spectra of SNe 2011hw and 2006jc were obtained 24 and 25 d after explosion, respectively, while that of SN 2002bj was obtained 7 d after its discovery, <2 weeks after the SN explosion. The vertical dashed lines mark the positions of the strongest He I features. The identification of other lines mentioned in the text has been done following Pastorello et al. (2007) and Anupama et al. (2009). All spectra were corrected for redshift, bringing them to the rest frame. The low signal-to-noise ratio 2013 September 9 spectrum of LSQ13ccw has been rebinned to 9 Å per bin.

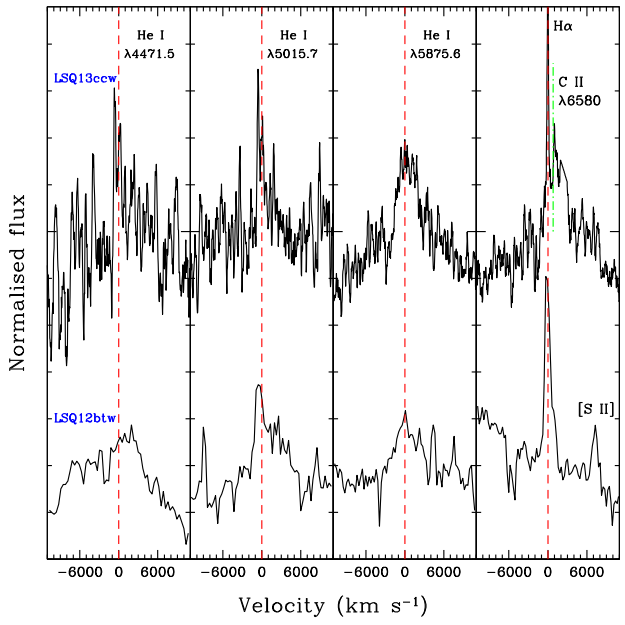

Figure 5. Profiles of three He I lines (λλ4471, 5016, 5876) and the Hα region in the Keck-II spectrum of LSQ13ccw obtained on 2013 September 9, and in the NTT spectrum of LSQ12btw obtained on 2012 April 12. Dashed red vertical lines in the four panels mark the zero-velocity position of the He I and Hα lines; the dot–dashed green line in the right-hand panel is centred at the average position of the C II λλ6578, 6583 doublet.

on the presence of relatively narrow P-Cygni absorptions in the He I features, blueshifted by about 2500 km s^{-1} from the rest wavelengths.

More controversial is the detection of Hα in the spectra of the two SNe. As stated before, in LSQ12btw the unresolved Hα is very likely produced by background contamination (right-hand panel of Fig. 5, and Fig. A1 in the appendix). In the case of LSQ13ccw, the situation is less clear. Very narrow Hα emission is visible in the 2013 September 10 Keck-II spectrum, but from the two-dimensional spectrum (Fig. A1) it is impossible to verify whether this line arises from the SN CSM or from the galaxy background. In addition, we cannot rule out that H contributes to the intermediate-velocity feature centred at about 6590 Å in the rest-wavelength spectrum, although this feature appears to be significantly redshifted (by about 30 Å) with respect to the Hα rest wavelength. In Fig. 5 (right-hand panel), the expected position of the core of the likely predominant C II λλ6578, 6583 emission is also marked. Accounting for these uncertainties, we tentatively suggest for LSQ13ccw a Type Ibn/IIn classification, although its putative Hα feature is slightly weaker than in other SNe Ibn/IIn, and much weaker than that observed in SNe IIn (see Pastorello et al. 2008b, 2015a; Smith et al. 2012, and comparison in Fig. 6).

Some similarity can be also noticed between the spectrum of LSQ13ccw and that of the enigmatic, fast-evolving SN Ib 2002bj (see Fig. 7, and Poznanski et al. 2010). The main differences are that the spectrum of SN 2002bj is dominated by lines having relatively broad P-Cygni profiles, with C II, S II and Si II features being

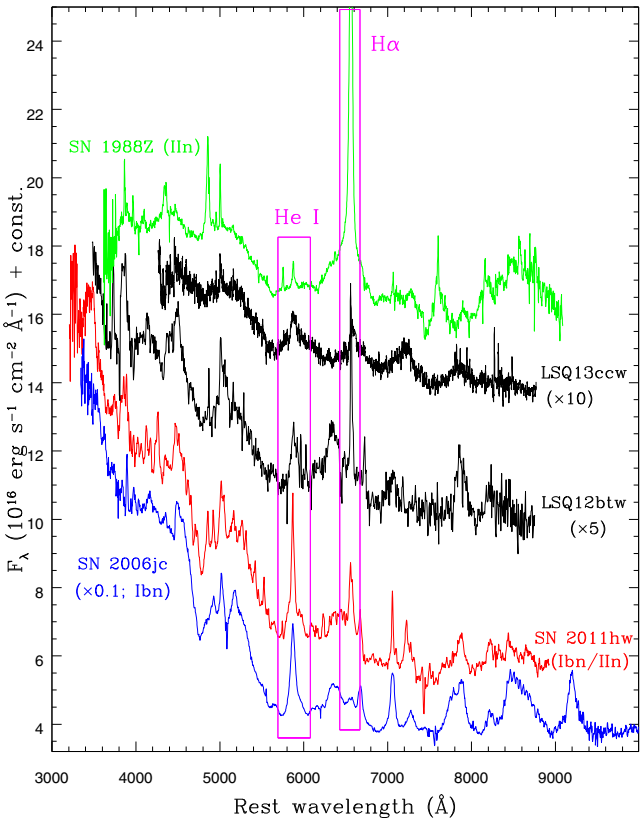

Figure 6. Comparison of the Keck-II spectrum of LSQ13ccw (obtained on 2013 September 9) and the NTT spectrum of LSQ12btw (obtained on 2012 April 12), with spectra of the Type Ibn SN 2006jc (Pastorello et al. 2007), the Type Ibn/IIn SN 2011hw (Pastorello et al. 2015a), and the prototypical SN IIn 1988Z (Turatto et al. 1993). The magenta boxes mark the regions of He I λ5876 and Hα in the five spectra.

unequivocally identified (in particular, Si II λ6355 is very prominent), and it does not show the depression at about 5600 Å typical of SNe Ibn, which is clearly visible in both LSQ13ccw and SN 2011hw. In the next section, we will address more comprehensively the implications of the similarity of some SNe Ibn with SN 2002bj.

In summary, the main spectral properties of the two SNe are those observed in other Type Ibn events (Figs 4, 6 and 7). Differences can be noticed, especially in the widths of the He I lines and in the spectral appearance of the region between 6300 and 6700 Å, that indicate a significant degree of heterogeneity in the ejecta/CSM composition. Differences are also observed in the strengths of the O I and Ca II features.

3 DISCUSSION

We have computed quasi-bolometric light curves, integrating the fluxes in the optical bands at all available epochs. When photometric points in individual bands were missing, their contribution was estimated by interpolating adjacent photometry. The contribution of the missing bands, especially at early epochs, was extrapolated assuming that the colour evolution of both LSQ12btw and LSQ13ccw were similar to those of other SNe Ibn observed at early phases (e.g. SNe 2000er and 2010al;[9] Pastorello et al. 2008a, 2015a).

The (optical) quasi-bolometric light curve of LSQ12btw is shown in Fig. 8 (top), along with those of SNe 2006jc (Foley et al. 2007; Pastorello et al. 2007, 2008a), 2010al and 2011hw (Pastorello et al. 2015a), and those of the Type Ib SN 1999dn (Benetti et al. 2011) and the luminous Type Ic SN 1998bw (Patat et al. 2001, and references therein). The peak luminosity of LSQ12btw, about 6×10^{42} erg s^{-1}, is high and comparable to those of other SNe Ibn and the 'hypernova' SN 1998bw. Although LSQ12btw is marginally fainter, its light curve is remarkably similar to that of SN 2006jc. In the same Fig. 8 (top), we also illustrate the 'UVOIR' curve (i.e. including the NIR contribution) of SN 2006jc (Foley et al. 2007; Pastorello et al. 2007, 2008a; Di Carlo et al. 2008; Immler et al. 2008; Mattila et al. 2008; Smith et al. 2008; Anupama et al. 2009). It was shown that in SN 2006jc, at phases >50 d, much of the flux moved to the NIR domain, owing to dust formation in a cool, dense circumstellar shell (e.g. Mattila et al. 2008; Smith et al. 2008). We do not have NIR observations to confirm a similar occurrence in LSQ12btw. Lacking observations at phases later than a few months, we cannot properly constrain the amount of ^{56}Ni synthesized by LSQ12btw. However, based on the striking photometric similarity with SN 2006jc, we argue that the two objects ejected similar amounts of ^{56}Ni (about 0.3 ± 0.1 M$_\odot$; e.g. Pastorello et al. 2008a).

In Fig. 8 (bottom), the quasi-bolometric light curve of LSQ13ccw (optical bands only) is compared with the corresponding light curves of SNe 2002bj and 2006jc. Although the evolution of SN 2006jc is fast in the optical bands (top of Fig. 8), one may notice that LSQ13ccw is even faster, declining in luminosity by two orders of magnitude in about 40 d. This rapid evolution is comparable with that experienced by the peculiar, still unique SN Ib 2002bj. However, the spectrum of SN 2002bj is somewhat different from that of LSQ13ccw and other SNe Ibn, since it shows hybrid characteristics between narrow-lined SNe Ia and SNe Ibn. Prominent P-Cygni lines of He I were detected in the early-time spectrum of SN 2002bj, together with more typical SN Ia features, such as Si II and S II (Poznanski et al. 2010) never unequivocally detected in SN Ibn spectra. Photometrically it is quite similar to an SN Ibn, with $M_R \approx -18.5$ mag at peak, and it has a similarly fast-declining light curve. Poznanski et al. (2010) suggested that some of the properties of SN 2002bj resemble those expected for the so called .Ia SNe[10] (Bildsten et al. 2007; Shen et al. 2010), but the arguments offered were not conclusive. Although the .Ia SN scenario is plausible for SN 2002bj, some similarity shared with SNe Ibn may suggest further exploration of the core-collapse scenario of massive stars as a viable explanation for this peculiar object.

So far, only 16 objects classified as SNe Ibn have been discovered, including LSQ12btw and LSQ13ccw (Table 4). Most of these objects show little or no evidence of hydrogen Balmer lines in their spectra, but do exhibit prevalent He lines of different widths, often with narrow components, and a blue pseudo-continuum likely caused by a blend of broad fluorescent lines of Fe. This suggests that SNe Ibn are powered by the interaction of SN ejecta with He-rich CSM, possibly produced during episodic mass-loss events affecting

[9] For these SNe, the synthetic photometry in the Sloan bands has been calculated using the available spectra.

[10] These were proposed to be produced in AM CVn-type binary white dwarfs, where a thermonuclear explosion occurs in the accreted He shell on the primary star, producing a fast and faint transient with a He-rich spectrum (Bildsten et al. 2007).

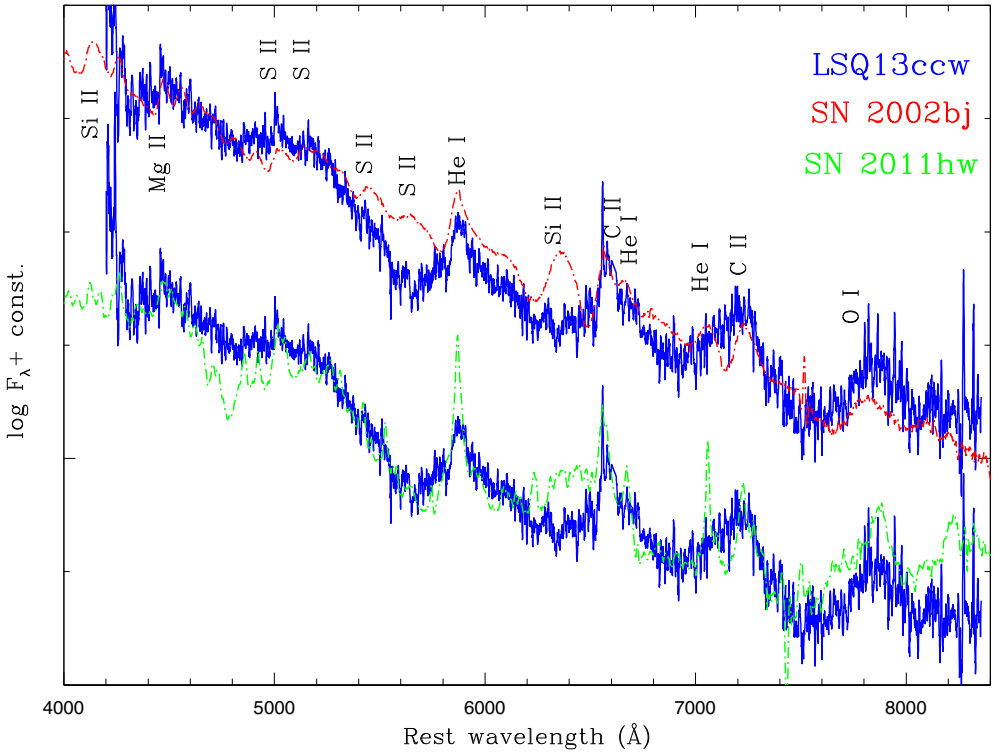

Figure 7. Comparison of the 2013 September 10 Keck-II spectrum of LSQ13ccw (blue solid line) with those of the peculiar SN Ib 2002bj (red dot–dashed line; top) and the Type Ibn/IIn SN 2011hw (green dot–dashed line; bottom). The most significant lines observed in the spectrum of SN 2002bj (Poznanski et al. 2010) are also marked.

the He-rich layers of the progenitor stars prior to the SN explosion. The precursors of SNe Ibn are likely H-poor WN-type or WCO-type Wolf–Rayet (WR) stars (Foley et al. 2007; Pastorello et al. 2007; Smith et al. 2008; Tominaga et al. 2008). Narrow H lines are clearly visible both in SN 2005la (Pastorello et al. 2008b) and SN 2011hw (Smith et al. 2012; Pastorello et al. 2015a), and link these events to massive stars still having a residual H layer. Smith et al. (2012) proposed that the precursor of SN 2011hw was indeed a star that was transitioning from a luminous blue variable (LBV) phase to an early WR phase. However, we argue that, since the H lines observed in the spectra of LSQ12btw and LSQ13ccw are weak or unrelated to the most recent progenitor evolution (cf. Section 2.2), their progenitors were H depleted at the time of explosion, and these events match a more canonical WN or WCO progenitor scenario.

Observations show a significant degree of heterogeneity within the Type Ibn SN family. In fact, the SN Ibn SN zoo includes objects with fast-evolving light curves (e.g. LSQ13ccw), and objects with a relatively broad light curve resembling those of normal stripped-envelope SNe (e.g. SN 2010al; Pastorello et al. 2015a). Some others even have double- or multipeaked light curves (SNe 2005la, 2011hw and iPTF13beo; Pastorello et al. 2008b, 2015a; Smith et al. 2012; Gorbikov et al. 2014), and at least one object having a very slow late-time luminosity evolution (OGLE-2012-SN-006; Pastorello et al. 2015b). This variety is probably related to intrinsic differences in the final properties of the progenitors and/or the configuration and composition of their CSM. The existence of transitional SNe Ibn showing evidence of circumstellar H (SN 2005la and 2011hw) suggests a continuity between stripped-envelope SNe and some SNe IIn (Turatto & Pastorello 2013). The diversity is also illustrated with the discovery of the first stripped-envelope event, SN 2010mb (Ben-Ami et al. 2014), that shows evidence of interaction with H-free CSM. Its spectra show narrow lines of α-elements (in particular, the collisionally excited [O I] λ5577 line) instead of the more canonical narrow H and He I lines.[11] This indicates that even He-free WR stars may experience significant mass-loss events a very short time before the terminal SN explosion.

3.1 SNe Ibn and their host environment

Thus far, it has never been properly investigated whether there is a connection between the occurrence of rare SNe Ibn, and chemical or morphological properties of their parent galaxies. Table 4 presents basic information on the host-galaxy properties for all 16 SNe Ibn, and we have homogenized the available (and sometimes sparse) data to common systems. The primary source of the morphological types was HyperLeda, and in a few cases NED or SDSS. In six cases, we relied on the deepest images collected during the follow-up campaigns carried out by our team (column 11). Distance moduli were obtained from the Virgo-corrected recessional velocities, assuming $H_0 = 73$ km s^{-1} Mpc^{-1}. In four cases,[12] we performed detailed photometric analyses to determine $B_{\rm tot}$, inclinations, and position angles required to derive the deprojected SN relative distances from the nuclei, $R_{0,\,\rm SN}/R_{25}$,[13] determined following Hakobyan et al. (2009). The total absolute magnitudes were estimated using the Galactic extinctions taken from Schlafly & Finkbeiner (2011), and the internal

[11] According to the SN classification criteria, an object with these characteristics should be formally designated an SN Icn.

[12] The galaxy parameters were determined for SNe 2011hw, LSQ13btw, OGLE-2012-SN-006 and iPTF13beo, CSS140421:142042+031602.

[13] R_{25} is the isophotal radius for the B-band surface brightness of 25 mag arcsec^{-2}.

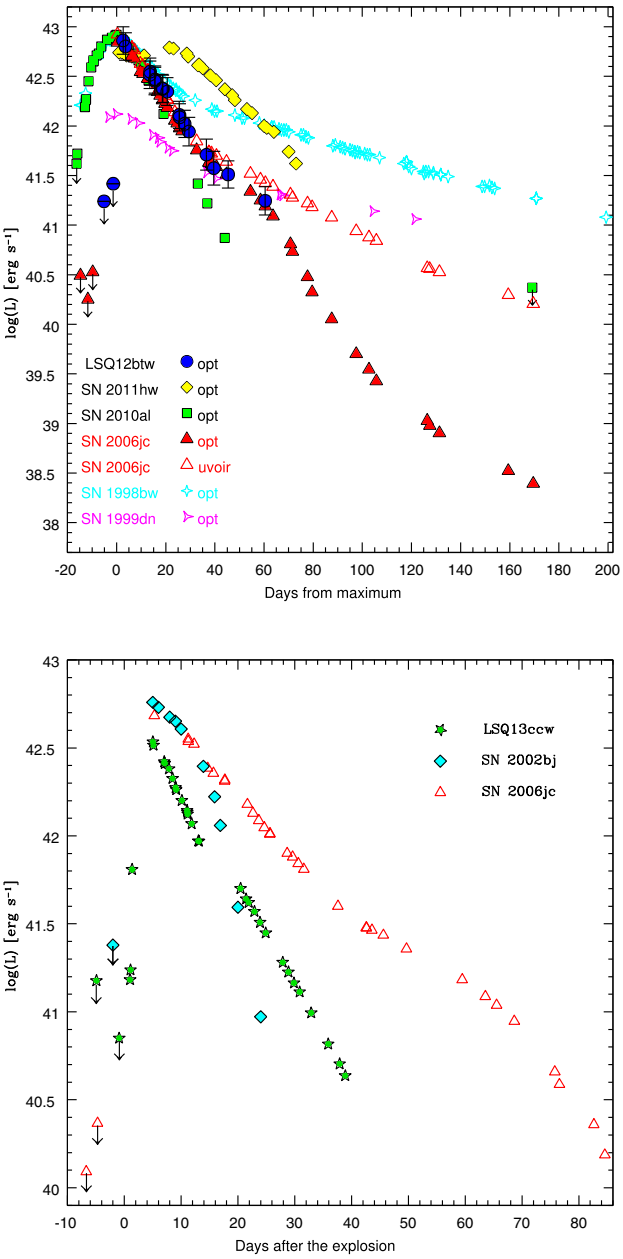

Figure 8. Top: quasi-bolometric light curve of LSQ12btw, computed integrating the fluxes in the *gVriz* optical bands compared with those of the Type Ibn SNe 2006jc, 2010al and 2011hw, the Type Ib SN 1999dn and the Type Ic SN 1998bw (computed integrating the *U*- to *I*-band fluxes; see the text for references). For SN 2006jc, the 'UVOIR' light curve obtained from integrating the optical plus NIR fluxes is also shown for comparison. Bottom: quasi-bolometric (*BVgri* bands) light curve of LSQ13ccw, compared with the curves of SNe 2002bj and 2006jc obtained by integrating the flux contributions of the *BVRI* bands. The stringent pre-discovery limits allow us to provide good constraints on the explosion epochs for the three objects.

absorptions from HyperLeda or computed with the same prescriptions. The average oxygen abundance estimates of the hosts (column 9) were computed according to the luminosity–metallicity relation of Tremonti et al. (2004). With the aim of disentangling possible effects due to radial gradients, we have also computed the metallicity at the SN radial distance. We assumed that Tremonti's metallicity is dominated by the contribution of the innermost regions of the host galaxy, and applied the average radial dependence of the oxygen abundance computed for the nearby sample of spiral galaxies of Pilyugin et al. (2004). The oxygen abundances at the distances of the SNe are reported in column 10 of Table 4.

Since none of the host galaxies are closer than the Virgo cluster, none have been studied in great detail. We note that among the 37 stripped-envelope CCSNe (SESNe, including SNe Ib/c and IIb) discovered during the decade 1999–2008 and closer than 30 Mpc (data from the Asiago Supernova Catalog), only SNe 2002ao and 2006jc exhibited easily recognizable He I emission features indicative of interaction with He-rich CSM. Therefore, it seems reasonable to assume that the relative discovery rate of SN Ibn/SESNe is ∼5.4 per cent, implying a relative ratio SN Ibn/CCSNe ≈2 per cent.

With a single notable exception, the galaxies hosting SNe Ibn are spirals, suggesting that these SNe are associated with young stellar populations. However, the discovery of the Type Ibn SN PS1-12sk (Sanders et al. 2013) poses new questions on the massive-star scenario for this class of objects. PS1-12sk exploded in the galaxy cluster RXC J0844.9+4258, in the outskirts of the luminous elliptical galaxy CGCG 208-042. The detailed analysis presented by Sanders et al. (2013) on the possible scenario involving degenerate progenitors still leaves some unclarified issues (e.g. presence of He, H, dense CSM, ejected ^{56}Ni mass, etc.). Though there is no direct evidence of star formation at the site of the explosion, the activity of the nucleus and the indications for the presence of cooling flows suggest that PS1-12sk is one of the rare (but known) cases of CCSNe exploding in early-type galaxies with some residual star formation activity (Hakobyan et al. 2008). On the other hand, the major outburst observed in SN 2006jc two years before the SN explosion can be comfortably explained with instabilities in massive stars during the final stages of their life (Smith & Arnett 2014), while it is hard to explain in a picture where the progenitor is a white dwarf.

The intrinsic luminosities of the host galaxies span a range of over 6 mag, from the dwarf hosts of OGLE-2012-SN-006 and SN 2006jc ($M_B \approx -15.8$ to -17.3 mag) to the bright spirals hosting SNe 2000er and 2014av ($M_B \leq -21.5$ mag). Such a wide luminosity range is reflected in a large spread of the integrated O abundances of the hosts (via the luminosity–metallicity relation of Tremonti et al. 2004) and the explosion sites (1.3 dex, column 10 of Table 4). The available information on the explosion sites, though scanty and based on statistical relations, thus seems to exclude the possibility that metallicity plays a significant role in determining the late-time evolution of the WR progenitors and their explosion as SNe Ibn.

In conclusion, a growing wealth of evidence indicates that the observed properties of SNe Ibn may be consistent with the explosion of massive WR (e.g. Foley et al. 2007; Pastorello et al. 2007; Tominaga et al. 2008) or transitional LBV/WR precursors (Smith et al. 2012; Pastorello et al. 2015a) that recently enriched their CSM with He-rich material through major eruptive events occurring shortly before the stellar core collapse, although we cannot rule out that binarity may play a significant role in the pre-SN evolution of the progenitor star. The sequence of events preceding core collapse is not fully understood and requires some fine tuning. We eagerly await the explosion of a very nearby SN Ibn, with direct information on the progenitor system, that will help solve the remaining open issues on the nature of this rare SN subclass.

ACKNOWLEDGEMENTS

This work is partially based on observations obtained under the ESO-NTT programmes with IDs 184.D-1140 and ID 188.D-3003,

Table 4. Basic information on the host galaxies of our SN sample.

SN	Galaxy	Type	z	μ (mag)	$B_{\rm tot}$ (mag)	$M_{\rm B,\,tot}$ (mag)	$R_{0,\,\rm SN}/R_{25}$	12+log(O/H) (dex)	12+log(O/H)$_{\rm SN}$ (dex)	Reference
1999cq	UGC 11268	Sbc	0.0271[a]	35.27	14.53	−21.52	0.13	9.24	9.18	A
2000er	PGC 9132	Sab	0.0302[a]	35.52	14.81	−21.68	0.52[b]	9.27	9.06	B
2002ao	UGC 9299	SABc	0.0054[a]	31.73	14.57	−18.07	0.60	8.60	8.36	B,C
2005la	KUG 1249+278	Sc	0.0190[a]	34.49	16.67	−18.32	0.94	8.64	8.27	D
2006jc	UGC 4904	SBbc	0.0061[a]	32.01	15.05	−17.29	0.70	8.45	8.17	B,C,E
2010al	UGC 4286	Sab	0.0172[a]	34.27	14.58	−20.44	0.37	9.04	8.89	F
2011hw	Anonymous	SBbc	0.023	34.92	16.02	−19.47	0.64	8.86	8.60	F,G
PS1-12sk	CGCG 208-042	E	0.0546[a]	36.84	15.50	−21.71	–	–	–	H
OGLE-2012-006[c]	Anonymous	Sd/Irr	0.057	36.94	21.33	−15.92	0.93	8.20	7.83	I,J
iPTF13beo	SDSS J161226.53+141917.7	Sp-ab	0.091	38.01	20.23[d]	−18.03	0.55	8.59	8.37	K
LSQ12btw	SDSS J101028.69+053212.5	Sab	0.0576	36.97	18.08[d]	−19.33	0.50	8.83	8.63	L
LSQ13ccw	PGC 866755	Sbc	0.0603	37.07	16.08	−21.29	0.92	9.19	8.83	L
CSS140421[c]	SDSS J142041.70+031603.6	–	0.07	37.41	20.46[d]	−17.27[e]	–	8.45	–	M
2014av	UGC 4713	Sb	0.0308[a]	35.56	14.09	−21.82	0.25	9.29	9.19	N
2014bk	SDSS J135402.41+200024.0	S	0.0697	37.40	19.52	−18.16	–	8.61	–	O
ASASSN-14dd	NGC 2466	Sc	0.0168[a]	34.22	13.72	−21.12	0.76	9.16	8.86	P,Q

Notes. After the SN and host-galaxy designations (columns 1 and 2), we report the galaxy type (column 3), the redshift (from the Virgo-infall-corrected recession velocity, when available; column 4), the distance modulus (assuming $H_0 = 73$ km s^{-1} Mpc^{-1}; column 5), the total B-band magnitude of the host galaxy (column 6), the absolute total B-band magnitude of the host galaxy corrected for Galactic (Schlafly & Finkbeiner 2011) and internal extinction and K-corrected following the HyperLeda prescriptions (column 7), the $R_{0,\,\rm SN}/R_{25}$ ratio (see text, column 8), the integrated oxygen abundance of the host galaxy following Tremonti et al. (2004, reported to the Tremonti $H_0 = 70$ km s^{-1} Mpc^{-1} scale, to simplify comparison; column 9), the oxygen abundance at the SN position assuming the average radial dependence as in Pilyugin, Vílchez & Contini (2004) (column 10), and the main references for the SN (column 11). Sources of information include HyperLeda, the NASA/IPAC Extragalactic Database (NED), and, when information was not available, our analysis of original frames (column 11).

A = Matheson et al. (2000); B = Pastorello et al. (2008a); C = Foley et al. (2007); D = Pastorello et al. (2008b); E = Pastorello et al. (2007); F = Pastorello et al. (2015a); G = Smith et al. (2012); H = Sanders et al. (2013); I = Prieto & Morrell (2013); J = Pastorello et al. (2015b); K = Gorbikov et al. (2014); L = this paper; M = Polshaw et al. (2014); N = Xu & Gao (2014); O = Morokuma et al. (2014); P = Stanek et al. (2014); Q = Prieto et al. (2014).

[a]Redshift computed from $v_{\rm Vir}$ (source Hyperleda). [b]Computed assuming $R_{0,\,\rm SN}$ equal to projected radius.

[c]OGLE-2012-006 = OGLE-2012-SN-006 and CSS140421 = CSS140421:142042+031602.

[d]Converted from Sloan magnitudes adopting the conversion relations from Lupton, 2005 (https://www.sdss3.org/dr8/algorithms/sdssUBVRITransform.php#Lupton2005).

[e]Adopting an average internal absorption $A_i = 0.2$ mag.

with the latter being part of PESSTO Survey. We are grateful to S. Bradley Cenko, Kelsey I. Clubb and WeiKang Zheng for their help with observations of LSQ13ccw at the Keck-II telescope, and to M. L. Pumo and S. Schulze for useful discussions.

AP, EC, SB and MT are partially supported by the PRIN-INAF (Istituto Nazionale di Astrofisica) 2011 with the project *'Transient Universe: from ESO Large to PESSTO'*. Research leading to these results has received funding from the European Research Council (ERC) under the European Union's Seventh Framework Programme (FP7/2007-2013)/ERC grant agreement no. [291222] (PI: SJS) and EU/FP7-ERC grant no. [307260] (PI: AG-Y). SJS is also supported by STFC grants ST/I001123/1 and ST/L000709/1. AG-Y is also supported by The Quantum Universe I-Core programme by the Israeli Committee for planning and funding, the ISF and GIF grants, and the Kimmel award. This research used resources of the National Energy Research Scientific Computing Center, which is supported by the Office of Science of the US Department of Energy under Contract No. DE-AC02-05CH11231. This work was partly supported by the European Union FP7 programme through ERC grant no. 320360. NER acknowledges support from the European Union Seventh Framework Programme (FP7/2007-2013) under grant agreement no. 267251 'Astronomy Fellowships in Italy'. AMG acknowledges financial support by the MICINN grant AYA2011-24704/ESP, by the ESF EUROCORES Program EuroGENESIS (MINECO grants EUI2009-04170), SGR grants of the Generalitat de Catalunya, and by the EU-FEDER funds. MDS gratefully acknowledges generous support provided by the Danish Agency for Science and Technology and Innovation realized through a Sapere Aude Level 2 grant. ST acknowledges support by the Transregional Collaborative Research Centre TRR 33 *'The Dark Universe'* of the DFG. AVF's supernova group at UC Berkeley received support through NSF grant AST–1211916, the TABASGO Foundation, Gary and Cynthia Bengier, the Richard and Rhoda Goldman Fund, and the Christopher R. Redlich Fund.

This paper is based on observations made with the Italian Telescopio Nazionale Galileo (TNG) operated on the island of La Palma by the Fundación Galileo Galilei of the INAF . It is also based on observations made with the LT and the GTC, operated on the island of La Palma at the Spanish Observatorio del Roque de los Muchachos of the Instituto de Astrofisica de Canarias. Some of the data presented herein were obtained at the W. M. Keck Observatory, which is operated as a scientific partnership among the California Institute of Technology, the University of California and the National Aeronautics and Space Administration (NASA). The Observatory was made possible by the generous financial support of the W. M. Keck Foundation. This work makes use of observations from the LCOGT network, and utilizes data from the 40-inch ESO Schmidt Telescope at the La Silla Observatory in Chile with the large-area QUEST camera built at Yale University and Indiana University.

The PS1 Surveys have been made possible through contributions of the Institute for Astronomy, the University of Hawaii, the Pan-STARRS Project Office, the Max-Planck Society and its participating institutes, the Max Planck Institute for Astronomy, Heidelberg and the Max Planck Institute for Extraterrestrial Physics, Garching, The Johns Hopkins University, Durham University, the University of Edinburgh, Queen's University Belfast, the Harvard–Smithsonian Center for Astrophysics, the Las Cumbres Observatory Global Telescope Network, Inc., the National Central University of Taiwan, the Space Telescope Science Institute, NASA under grant no. NNX08AR22G issued through the Planetary Science Division of the NASA Science Mission Directorate, the US NSF under grant AST–1238877, and the University of Maryland.

This research has made use of the NASA/IPAC NED which is operated by the Jet Propulsion Laboratory, California Institute of Technology, under contract with NASA. We acknowledge the usage of the HyperLeda data base (http://leda.univ-lyon1.fr).

REFERENCES

Anupama G. C., Sahu D. K., Gurugubelli U. K., Prabhu T. P., Tominaga N., Tanaka M., Nomoto K., 2009, MNRAS, 392, 894
Baltay C. et al., 2013, PASP, 125, 683
Ben-Ami S. et al., 2014, ApJ, 785, 37
Benetti S. et al., 2011, MNRAS, 411, 2726
Bianco F. B. et al., 2014, ApJS, 213, 19
Bildsten L., Shen K. J., Weinberg N. N., Nelemans G., 2007, ApJ, 662, L95
Chugai N. N., 2009, MNRAS, 400, 866
Di Carlo E. et al., 2008, ApJ, 684, 471
Filippenko A. V., 1982, PASP, 94, 715
Filippenko A. V., 1997, ARA&A, 35, 309
Foley R. J. et al., 2007, ApJ, 657, L105
Fraser M. et al., 2013a, MNRAS, 433, 1312
Fraser M. et al., 2013b, ApJ, 779, L8
Gorbikov E. et al., 2014, MNRAS, 443, 671
Graham M. L. et al., 2014, ApJ, 787, 163
Hadjiyska E. I., Rabinowitz D., Baltay C., Zinn R., Coppi P., Ellman N., Miller L. R., 2011, BAAS, 217, 433.18
Hakobyan A. A., Petrosian A. R., McLean B., Kunth D., Allen R. J., Turatto M., Barbon R., 2008, A&A, 488, 523
Hakobyan A. A., Mamon G. A., Petrosian A. R., Kunth D., Turatto M., 2009, A&A, 508, 1259
Immler S. et al., 2008, ApJ, 674, L85
Inserra C. et al., 2013, ApJ, 770, 128
Jester S. et al., 2005, AJ, 130, 873
Kangas T. et al., 2013, Astron. Telegram, 5380, 1
Landolt A. U., 1992, AJ, 104, 340
Margutti R. et al., 2014, ApJ, 780, 21
Matheson T. et al., 2000, AJ, 119, 2303
Mattila S. et al., 2008, MNRAS, 389, 141
Mauerhan J. C. et al., 2013, MNRAS, 430, 1801
Maund J. R. et al., 2006, MNRAS, 369, 390
Modjaz M. et al., 2014, AJ, 147, 99
Morokuma T. et al., 2014, Cent. Bur. Astron. Telegrams, 3894, 1
Nozawa T. et al., 2008, ApJ, 684, 1343
Ofek E. O. et al., 2013, Nature, 494, 65
Pastorello A. et al., 2007, Nature, 447, 829
Pastorello A. et al., 2008a, MNRAS, 389, 113
Pastorello A. et al., 2008b, MNRAS, 389, 131
Pastorello A. et al., 2013, ApJ, 767, 1
Pastorello A. et al., 2015a, preprint (arXiv:1502.04946)
Pastorello A. et al., 2015b, preprint (arXiv:1502.04946)
Patat F. et al., 2001, ApJ, 555, 900
Paturel G. et al., 2003, A&A, 412, 45
Pilyugin L. S., Vílchez J. M., Contini T., 2004, A&A, 425, 849
Polshaw J. et al., 2014, Astron. Telegram, 6091, 1
Poznanski D. et al., 2010, Science, 327, 58
Prieto J. L., Morrell N., 2012, Astron. Telegram, 4734, 1
Prieto J. L. et al., 2014, Astron. Telegram, 6293, 1
Sakon I. et al., 2009, ApJ, 692, 546
Sanders N. E. et al., 2013, ApJ, 769, 39
Schlafly E. F., Finkbeiner D. P., 2011, ApJ, 737, 103
Shen Y., Kasen D., Weinberg N. N., Bildsten L., Scannapieco E., 2010, ApJ, 715, 767
Smartt S. J. et al., 2013, The Messenger, 154, 50
Smith N., Arnett W. D., 2014, ApJ, 785, 82
Smith J. A. et al., 2002, AJ, 123, 2121
Smith N., Foley R. J., Filippenko A. V., 2008, ApJ, 680, 568
Smith N. et al., 2009, ApJ, 695, 1334
Smith N. et al., 2012, MNRAS, 426, 1905
Stanek K. Z. et al., 2014, Astron. Telegram, 6269, 1
Tartaglia L. et al., 2015, MNRAS, 447, 117
Tomasella L. et al., 2014, Astron. Nachr., 335, 841
Tominaga N. et al., 2008, ApJ, 687, 1208
Tonry J. L. et al., 2012, ApJ, 750, 99
Tremonti C. A. et al., 2004, ApJ, 613, 898
Turatto M., Pastorello A., 2013, in McCray R. A., Ray A., eds, Proc. IAU Symp. 296, Supernova Environmental Impacts. Cambridge Univ. Press, Cambridge, p. 63
Turatto M., Cappellaro E., Danziger I. J., Benetti S., Gouiffes C., Della Valle M., 1993, MNRAS, 262, 128
Valenti S. et al., 2012, Astron. Telegram, 4037, 1
Van Dyk S. et al., 2000, PASP, 112, 1532
Xu Z., Gao X., 2014, Cent. Bur. Electron. Telegrams, 3865, 1
Yaron O., Gal-Yam A., 2012, PASP, 124, 668

APPENDIX A: NARROW LINES IN THE SPECTRA OF LSQ12BTW AND LSQ13CCW

In Fig. A1, we show a close-up view of the Hα region in our highest-resolution, two-dimensional spectra of LSQ12btw and LSQ13ccw. In the spectrum of LSQ12btw, narrow Hα, [N II] and [S II] are detected, with a spatial extension which is broader than the SN emission. For this reason, we believe that these lines are physically unrelated to the SN. In the spectrum of LSQ13ccw, the narrow Hα emission does not show spatially extended wings broader than the continuum. Therefore, in this case we cannot firmly establish or rule out the association of this feature with the SN.

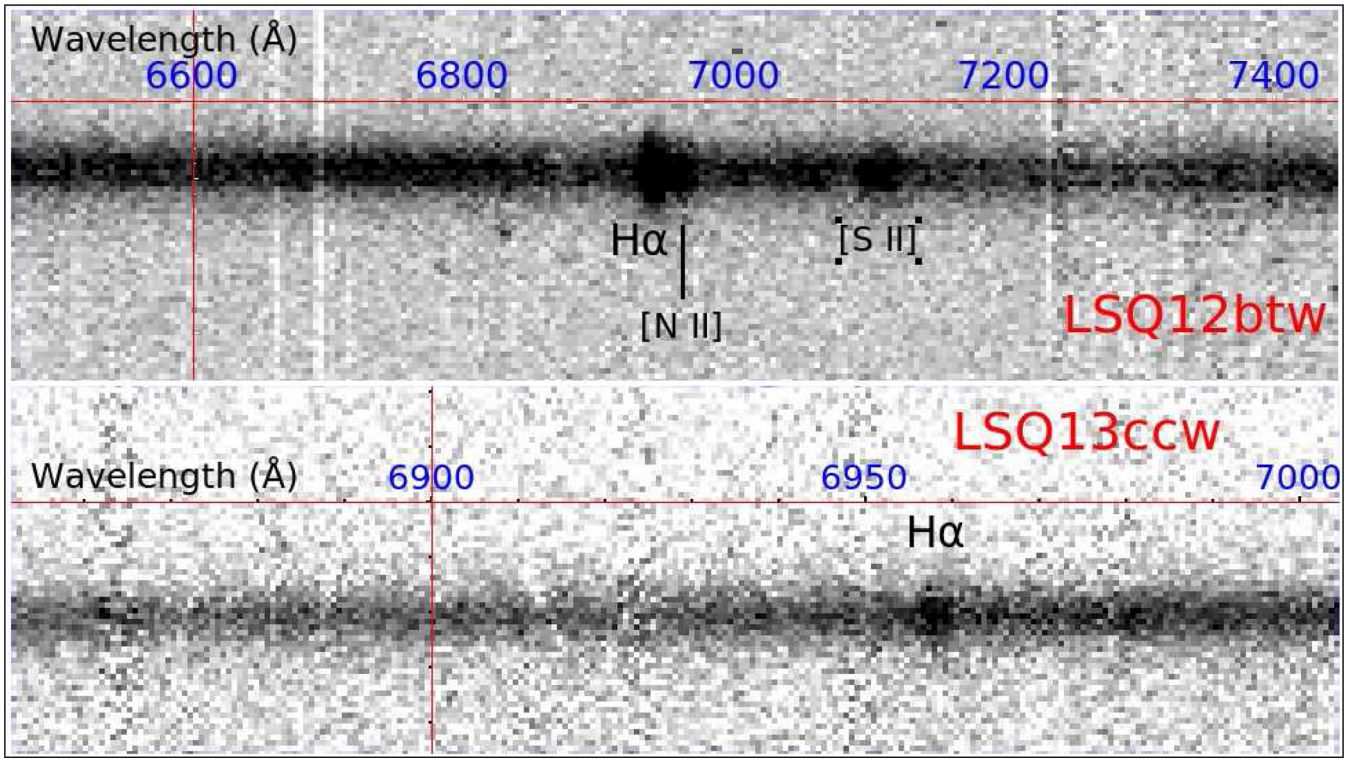

Figure A1. Zoom-in on the Hα region in the highest-resolution two-dimensional spectra of the two SNe: NTT spectrum of LSQ12btw taken on 2012 August 21 (top) and Keck-II spectrum of LSQ13ccw obtained on 2013 September 9 (bottom). Both spectra are shown at the host-galaxy frame.

[1]*INAF–Osservatorio Astronomico di Padova, Vicolo dell'Osservatorio 5, I-35122 Padova, Italy*
[2]*Department of Physics, Yale University, PO Box 208120, New Haven, CT 06520-8120, USA*
[3]*Las Cumbres Observatory Global Telescope Network, Inc., Santa Barbara, CA 93117, USA*
[4]*Department of Physics, University of California, Santa Barbara, CA 93106-9530, USA*
[5]*Max-Planck-Institut für Astrophysik, Karl-Schwarzschild-Str. 1, D-85741 Garching, Germany*
[6]*INAF–Osservatorio astronomico di Capodimonte, Salita Moiariello 16, I-80131 Napoli, Italy*
[7]*Physikalisches Institut, Universität Bonn, Nußallee 12, D-53115 Bonn, Germany*
[8]*Department of Astronomy, University of California, Berkeley, CA 94720-3411, USA*
[9]*Institute of Astronomy, University of Cambridge, Madingley Road, Cambridge CB3 0HA, UK*
[10]*Department of Particle Physics and Astrophysics, Faculty of Physics, The Weizmann Institute of Science, Rehovot 76100, Israel*
[11]*Astrophysics Research Centre, School of Mathematics and Physics, Queen's University Belfast, Belfast BT7 1NN, UK*
[12]*Institut de Ciències de l'Espai (CSIC-IEEC), Campus UAB, Torre C5, 2a planta, E-08193 Barcelona, Spain*
[13]*Computational Cosmology Center, Computational Research Division, Lawrence Berkeley National Laboratory, 1 Cyclotron Road MS 50B-4206, Berkeley, CA 94720, USA*
[14]*Department of Physics and Astronomy, Aarhus University, Ny Munkegade 120, DK-8000 Aarhus C, Denmark*
[15]*School of Physics and Astronomy, University of Southampton, Southampton SO17 1BJ, UK*
[16]*European Organisation for Astronomical Research in the Southern Hemisphere (ESO), Karl-Schwarzschild-Str. 2, D-85748 Garching bei München, Germany*

This paper has been typeset from a TEX/LATEX file prepared by the author.